Research Paper   Open Access

Performance Evaluation of a Newly Constructed Three Phase Flexible Inverter for Speed Control of a Brushless Dc Motor

Nyong-Bassey Bassey Etim

Department of Electrical/Electronics Engineering, Federal University of Petroleum Resources Effurun, Nigeria

Abstract: *This paper presents the analysis of a real-time experimental and simulation results from a series of tests performed on a newly constructed three phase flexible invertercapable of operating in two modes; DC-AC inverter or DC-DC converter. A control algorithm is used to select one of the pre-programmed mode, where one of which may be applied for variable speed control of a three phase brushless DC (BLDC) motor. The inverter generates three pairs of unequal but fixed duty cycle pulse width modulation (PWM) pulses at a constant frequency which may be varied. The inverter as a single variable DC power supply and a single variable AC supply has also been simulated in MATLAB/SIMULINK software to investigate the effect of motor and control parameter variation such as Motor load inductance, duty cycle of the reference input and the triangular wave carrier frequency respectively.*

Keyword: BLDC motor, Flexible inverter, H-Bridge, PWM, Speed Control,

I. Introduction

According to [1], The Control of electric motor is one of the broad areas where power electronics plays an important role. Brushless DC motor is often incorporated in digitally controlled systems design where servo-type application is needed for the control of speed, position and torque [2]. The wear and tear associated with the mechanical commutation of a permanent-magnet dc motor which is similar to the brushless DC motor (BLDC) is avoided since it utilizes solid-state electronic switches to achieve commutation hence increasing its reliability [1, 3,4]. In [3] dsPIC30F chip by Microchip Technology Incorporatedis utilized with reasons being that it integrates a Micro controller (MCU) and DSP chip specifically designed for motor control and has wide acceptance in the global market. The speed control of BLDC motor entails varying the motor phase voltages and can be achieved by pulse amplitude modulation, pulse width modulation or hysteresis control.

The BLDC motor as an adjustable speed drive controlled by PWM technique promises high energy efficiency.

This paper focuses on the results of three important series of comprehensive tests performed on a newly constructed three phase flexible inverter in order to ensure proper operability. Also the effect of varying circuit parameters are simulated using MATLAB/SIMULINK.

II. Flexible Inverter Principle of Operation

The flexible inverter has two programmable operating modes; as a 3-phase DC-AC inverter and a DC-DC converter thus its operation depends on which mode is initialized. The inverter operates by using a dsPIC130F3010 microcontroller to generate a sequence of pulse width modulation (PWM) pulses used to drive the IR2130 MOSFET driver chip. The driver chip in-turn switches on/off (with 24V / 0V DC) the gates of three MOSFET pairs consecutively to drive the 3-phase brushless DC motor.The 120° phase sequence of commutation which is used to drive the MOSFET depends on the rotor position which is sensed by three Hall Effect sensors and the result fed back to the PIC microcontroller. The MCU determines the rotor position and applies the corresponding commutation sequence to the switching devices, energizing the armature windings stator in sequence and inducing magnetic field which causes the rotor to rotation. The MCU peripheral circuit diagram is shown in Figure 1.The rotor position is sensed constantly and the update used determine the commutation sequence used to alter the armature windings state [3, 5]. The schematic diagram of the flexible inverter for control of BLDC motor speed is shown in Figure 2.

The first test was the PWM Pulse test which investigated the parameters such as the frequency, the duty cycle, dead time and gate on voltage (V_{GS}) of the three pairs of fixed duty cycle PWM pulses at constant frequency generated by the PIC microcontroller to ascertain if the inverter was functioning properly.In the second test, the

inverter was operated as a three phase sine-wave generator and parameters such as the peak current, RMS current and power dissipated by the motor were determined. Test three involved the brushless DC motor control which investigated the effect of altering the potentiometeralong its extremes which in turn increased and decreased the frequency of the pulse width modulation pulses respectively with the speed of the motor reduced and increased accordingly. The potentiometer setup is in a voltage divider configuration with the output voltage fed into the PIC which performs analogue to digital conversion (ADC) by mapping the range of output voltages controlled by the potentiometer to a range of pre-defined valueswhich is used to vary the frequency of the pulse width modulation (PWM) pulses [6,11].

The inverter as a single variable DC power supply and a single variable AC supply was simulated using MATLAB/ Simulink software to investigate the effect of varying the motor load inductance, duty cycle of the reference input and the triangular wave carrier frequency.

III.Fixed PWM Pulse Test

Before the PWM pulse test was carried out, the constructed board passed through an initial error check to ensure that the board supplied +5V DC and +15VDC. The power supply circuit is shown in Figure 3. Haven passed the error check test, the constructed board was connected to the power supply and also interfaced to a desktop computer through a MPLAB interface box which was connected to the R22 port. The PWM pulse test was activated on the PIC Chip through the MPLAB ICD 2 software interface and compiled and loaded on the PIC Chip afterwards. This activated the PWM pulse test. The six output voltages from the microcontroller which switches the MOSFET H-Bridge to produce the gate signals which were measured in pairs, J1&J2, J3&J4, J5&J6 using the oscilloscopetrace as shown in Figure 4a and 4b. The Gate on Voltage from the oscilloscope reading was observed and documented. Table I shows the Amplitude of the Voltage, Time on and off PWM frequency and duty cycle, and dead time.

For the three pairs of PWM pulse, PWM frequency was calculated using following formula:

Frequency (Hertz) =1 / (Period)   (1)

Period (T) = Time on + Time off   (2)

J1:$1/ ((12.06 + 86.77) *10^{-6}Seconds)$ = 10.11 KHz

For the three pairs of PWM pulses, Duty Cycle was also calculated using the following formula:

*Duty cycle = (Time on/ Period) *100%*J1:*12.06 µS / (12.06µS + 86.77 µS)* 100 = 12.2%*

The dead time for each pair of gate signal was observed from the oscilloscope trace. It is the time lag in the order of 410nS between the Hi and Lo side device switching on and off respectively [7]. The importance is to prevent short circuiting in the inverter which may lead to a permanent damage. Also from the oscilloscope trace it was observed that each gate square pulse had a constant frequency of 10.1 KHz while the duty cycle for each gate signal pulse was different but fixed for the entire period. This confirms that the inverter passed the fixed PWM pulse test and operatedcorrectly [8].

IV. Three Phase Sine Wave Test

Using MPLAB software, the Frequency test mode on the PIC was activated and the PWM pulse test was deactivated because only one mode be activated at a time. The flexible inverter was connected to a RL load which is an equivalent motor loadas shown in Figure 5. The power supply unit was limited to 24V - 1A, and the voltage difference of V1 and V2 was captured using math function in the oscilloscope. Figure 6 shows the scope trace capturing the voltage difference across the 47Ω resistor in order to determine the current flowing through the inductor which represents the coil windings in a RL load model.The resulting current is plotted and shown in Figure 7.

The potentiometer R22 was altered within its extremes and the effect on the PWM voltage and frequency was observed and captured using the oscilloscope. The maximum frequency was 19.72 Hz and the minimum frequency was 1.93 Hz as captured from the scope trace in Figures8 and 9 respectively.

From Figure 7, the peak current value is 0.162 A. The rms current value was calculated using the formula:

Rms current (I_{rms})= peak current /√2   (3)

Rms voltage (V_{rms}) = peak voltage/√2   (4)

$I_{rms} = 0.162/√2 = 0.114A$and $V_{rms} = 7.65/√2$=5.4V

The power dissipated into the load was determined using the formula:

Power (P)= I_{rms} *V_{rms} (5)

P= 0.114 x 5.40 = 0.615W

V. Brushless DC Motor Control Test

The inverter was used to drive and control the speed of a three phase, 8 poles brushless DC motor. The code for this mode was activated and loaded unto the PIC. The relationship of altering the potentiometer along its extremes with respect to the effect it has on the speed of the brushless DC motor, duty cycle, voltage amplitude and frequency were investigated with scope traces captured and shown in Figures 10and 11 .The calculated motor speed corresponding to supply frequency is presented in Table II.

The Formula used for calculating the Speed of the BLDC Motor is

Motor Speed, n_s(rpm)= 120 x Supply frequency (f_s) /Number of Motor pole (P)(6)

From Table II, The BLDC motor speed range of is from 755 rpm – 2556 rpm
Also to run the motor at 2000 rpm the supply frequency will be:
*Supply frequency (f_s) =(n_s * P) /120 = (2000 * 8)/120 = 133.33 Hz*

The Scope trace fromFigure 10, was capture when the motor ran at 2017 rpm with supply frequency of 134.48 Hz as against 2000 rpm and corresponding frequency of 133.33 Hz because of over sensitivity of potentiometer which varied the frequency range. Also the frequency values fluctuated rapidly on the oscilloscope screen which made it difficult to capture the trace at 133.33Hz. From Figure 11 which shows the time on and period the Duty Cycle was calculated as follows:

Duty Cycle (D) = Time on /Period   (7)
D = 3.72/(3.72 + 3.71) μs * 100 = 50%

The potentiometer was altered to run the motor at maximum speed which was 2556 rpm occurring at a maximum frequency of 170.42 Hz. The duty cycle was calculated from the resulting scope trace.
Duty Cycle = Time on/Period
= 2.91/ (2.91 + 2.95) μS* 100 = 49%

As observed it can be stated that the Duty cycle corresponding to the maximum frequency which runs the motor at a maximum speed of 2556 rpm is 49 percent, while, the duty cycle corresponding to the motor speed of 2017 rpm at a frequency 133.33Hz is 50 percent. The values for the duty cycles with varying frequency (or period) are equal when rounded off. Theoretically, the fixed duty cycles should be exactly the same. However, this is not the case as the MOSFET is not an ideal switch when dealt with practically [1]. Also observing the duty cycle when the motor ran at a low speed of 755rpm which occurred at the lowest frequency, 53.3Hz, the duty cycle was 50 percent. This confirms the inverter supplies fixed duty cycle pulse width modulation (PWM) pulses despite the varying frequency. Also it was observed that altering the potentiometer along its extremes varied the period of the PWM pulses and in turn varied the speed of the motor to achieve 'the motor control'.
The PIC microcontroller performs Analogue to digital conversion by reading the value of the output voltage by (external analogue signal) of the voltage divider circuit which is controlled by R22 potentiometer. This value is read and used to determine the value of the periodfor the generated PWM pulses accordingly. An increase in frequency increases the motors rotational speed while a decrease in the frequency decreases the motor rotational speed. According to [1], the mean power delivered to the motor can be controlled by keeping the on time constant while varying the period of the pulse width modulation pulses. This however, confirms that the potentiometer R22 functions as a controller of motor electromagnetictorque [10].
By measuring hall sensors, H1, H2, and H3 on the inverter and analyzing the scope trace in Microsoft ® Excel the 3 bit Hall Effect Sensor sequence was determined. The result obtained in Figure 9 correlates the fact that the Hall sensors are positioned 120° electrical apart. For the microcontroller to drive the MOSFETs, a 3-bit Hall sensor sequenceasa result of sensing the position of the rotor is generated and read by the microcontroller at high processing speed. The Microcontroller generates a 120 ° phase shift commutation sequence in response to switch the MOSFETs on and off. In Table III a six state commutation sequence for both clockwise and anticlockwise rotation was derived fromthe 3-bit Hall Effect sensor sequence.The Hall sensor 3-Phase voltage is shown in Figure 12 and analyzed in Microsoft Excel to deduce the 3-bit Hall Effect sensor sequence shown in Figure 13.As observed during commutation two phases are switched on the third phase is off [4, 10, 12].The picture of the flexible inverter circuit board is shown in Figure 14 and also the BLDC motor speed control flow chart diagram is shown in Figure 15.

VI. Flexible Inverter Simulation

A. Variable DC Supply

The flexible inverter was modelled and simulated in SIMULINK as shown in Figure 16 as a single phase variable DC power supply with fixed duty cycle pulse width modulation pulses. RL Load impedance which is

analogous to a motor load was supplied by the Variable DC power supply. The triangular wave carrier was set to have a frequency of 20 KHz with varying amplitude of 0 and +1, and reference inputvalue of 0.5 corresponding to 50 percent duty cycle. The load has a resistance of 47Ω with and inductance of 3.3mH. The output waveform obtained is shown in Figure 17.From the observation of Figure 17the output current waveform is follows an exponential fundamental however chattering caused by the triangular carrier wave used for Pulse Width Modulation is observed. There is an exponential rise as a result of the inductance load which opposes a change in current before attaining steady state. From 0 mS to 0.3 mS there is an exponential rise and after 0.3mS steady state is attained with corresponding peak current of 0.3A. At steady state there is undulation between 0.2A and 0.3A. The steady state current is 0.25A. Also the effect of changing the reference input value, varying the triangular wave carrier frequency, and the load inductance value was investigated.

From Figure 18, it was observed that the effect of decreasing the reference input values (from 1 to 0.5 and from 0.5 to 0.2) caused the peak value of the output current to also decrease (from 0.5A to 0.3A and to 0.06A). From Figure 19, the effect of decreasing the load inductance (from 10mH to 3.3mH and from 3.3mH to 1mH) caused the peak value of the output current to increase (from a value of 0.267A to 0.30A and to 0.39A) with a faster rise time. While the effect of decreasing the triangular carrier wave frequency (from 100 KHz to 50 KHz and to 10 KHz) caused the peak value output current to increase (from 0.25 A to 0.27 A and then to 0.46 A) as observed from Figure 20.

B. Variable AC Power Supply

The flexible inverter was also simulated as a single phase varying AC supply. The triangular carrier waveform was set to vary between -1 and +1 at10 KHz with a reference input of 50Hz.The effect of increasing the sine wave input frequency from 50Hz to 100 Hz caused the number of cycles to double when simulated for an equal period of time as shown in Figures 21 and 22.

The effect of increasing the load inductance from 3.3mH to 33mH, caused the peak current to fall from 0.36A to 0.26A as shown in Figure 21 and Figure 23 respectively. Hence, since Inductor impedes change in current the greater the inductance the greater the opposition to current change and hence the result of a lower peak current value.

VII. Conclusion

Series of tests have been carried out to investigate the proper operations of a three phase inverter as a variable frequency AC source used for controlling the speed of a three phase brushless DC motor. The Flexible inverter component list is shown in Table IV. From the test results obtained, it was confirmed that the inverter generates three pairs of unequal but fixed pulse width modulation (PWM) pulses at a constant frequency. The frequency of the pulse width modulated PWM pulses is controlled by altering the R22 potentiometer along its extreme which consequently determines the rotational speed when used to control a brushless DC motor. Also the single phase inverter was modelled and simulated in SIMULINK as a variable AC and DC power supply and RL load (motor winding equivalent). From the simulation results it was confirmed that the effect of altering the reference input value and triangular wave carrier frequency used to generate the PWM and/or load inductance pulses caused the output current peak value to vary.

Table I. Results showing observed and calculated parameters for the three pairs of gate pulses

PIC Output & Gate Signal	Gate on Voltage (V)	Time on (μS)	Time off (μS)	PWM frequency (KHz)	PWM Duty Cycle %	Dead time (nS)
J1	5.2	12.06	86.77	10.11	12.2	410
J2	5.2	85.96	12.88	10.11	86.9	410
J3	5.2	44.20	54.62	10.11	44.7	410
J4	5.2	53.80	45.20	10.10	54.3	410
J5	5.3	24.44	74.38	10.11	24.7	410
J6	5.2	73.58	25.24	10.11	74.4	410

Table II.
Calculated motor rotational speed range while connected to the 3 phase inverter.

Supply frequency f_s (Hz)					
	50.33	90	133.33	134.44	170.42
Motor Speed (rpm)	755	1350	2000	2017	2556

Table III. Commutation table for clockwise and counter clockwise rotation

Commutation Sequence #	Sequence for Clockwise Rotation						Sequence for Counter Clockwise Rotation					
	Hall Sensor Input			Phase Current			Hall sensor Input			Phase Current		
	H1	H2	H3	A	B	C	H1	H2	H3	A	B	C
1	1	0	0	DC+	DC-	OFF	1	0	0	DC+	OFF	DC-
2	1	1	0	DC+	OFF	DC-	1	0	1	DC+	DC-	OFF
3	0	1	0	OFF	DC+	DC-	0	0	1	OFF	DC-	DC+
4	0	1	1	DC-	DC+	OFF	0	1	1	DC-	OFF	DC+
5	0	0	1	DC-	OFF	DC+	0	1	0	DC-	DC+	OFF
6	1	0	1	Off	DC-	DC+	1	1	0	OFF	DC+	DC-

Table IV. List of Flexible Inverter Components

S/N	Component Name	Rating
1	R1, R20	1KΩ
2	R2, R3, R4	4.1 KΩ
3	R9, R18, R19	1 KΩ
4	R11 – R17	0.1 KΩ
5	R0, R10, R24	0.003 KΩ
6	R13	5 KΩ
7	R25	39 KΩ
8	MOSFET U10 – U15	IRF540
9	D1, D2	IN4148
10	C23	1μF
11	C7	220uF
12	C11 – C13	10μF
13	C14, C15	220μF
14	U3 -U5, U7	UF4001GP
15	U8,U9	LM7805C7
16	R22	10 KΩ
17	C1-C3	10nF
18	C4, C5,C10, C16, C26	100nF
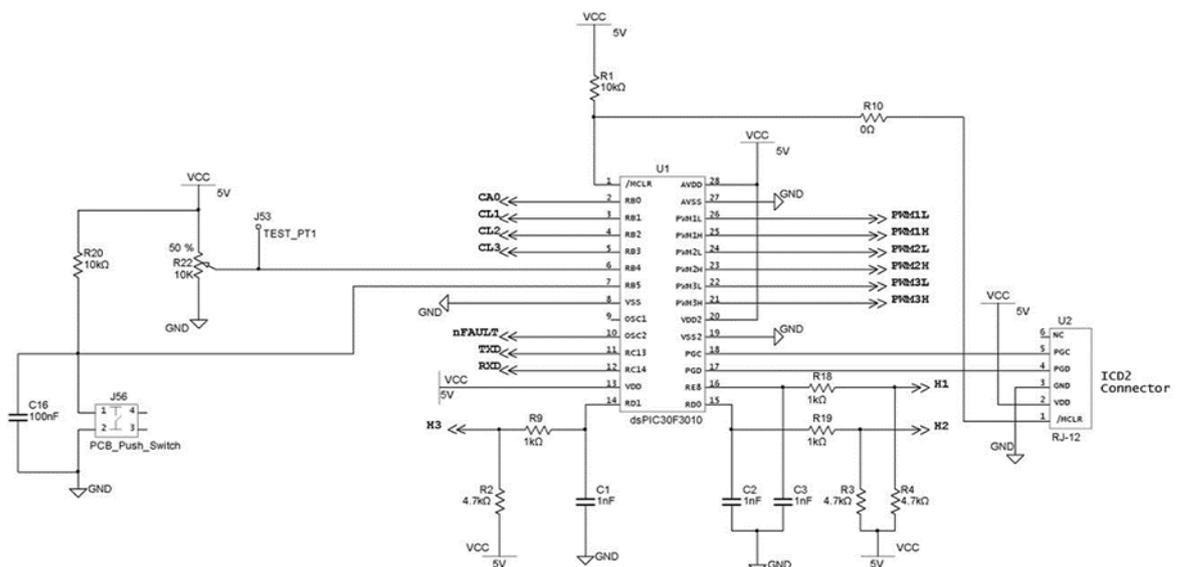
Fig. 1 dsPIC130F3010 PeripheralCircuit Diagram
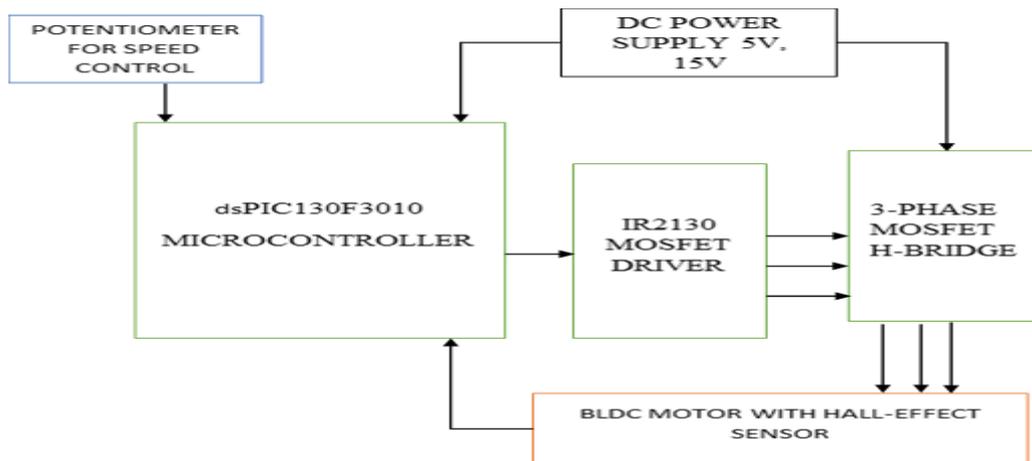
Fig 2. Schematic Diagram ofFlexible Inverter Control of BLDC Motor Speed
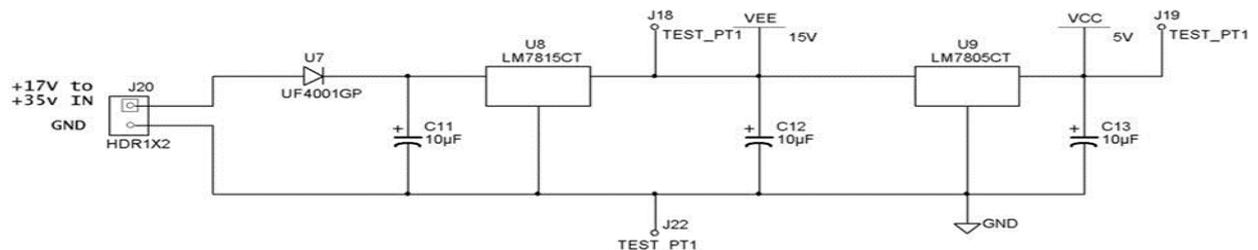
Fig 3. Power Supply circuit
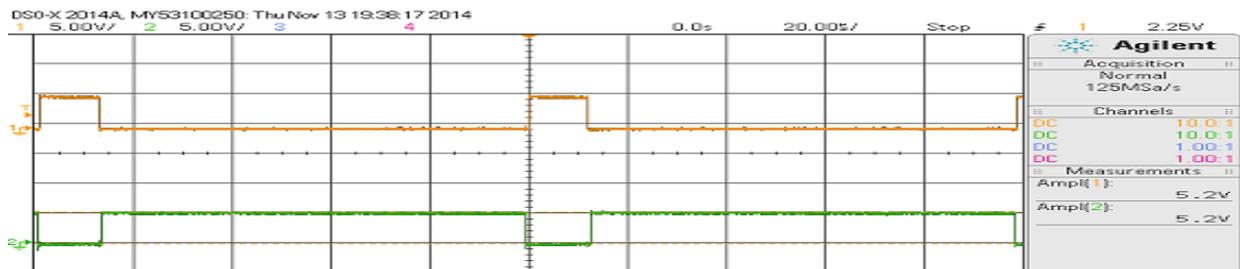
Fig 4a. A pair of PWM pulse fed into the J1 & J2 ofMOSFET H-Bridge
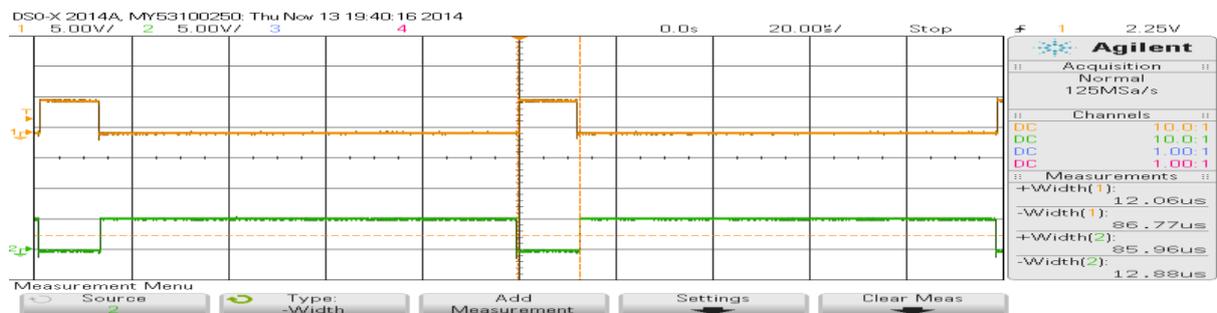
Fig 4b. A pair of PWM pulse fed into the J1 & J2 ofMOSFET H-Bridge
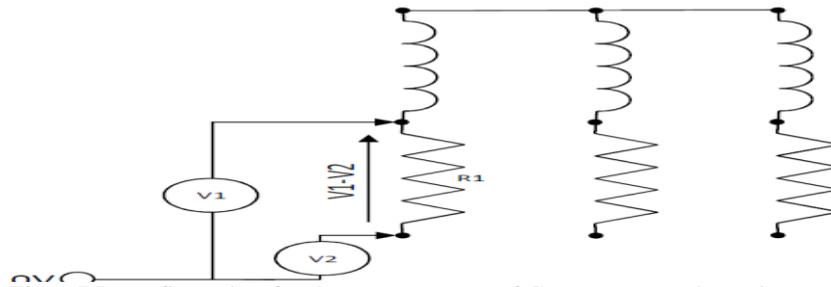
Fig 5. RL configuration for the measurement of Current across the resistor.
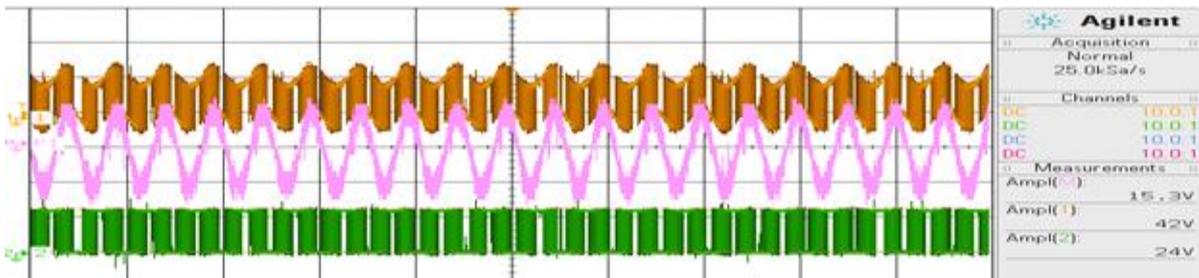
Fig6. Oscilloscope trace for V1, V2 & V1-V2 voltage
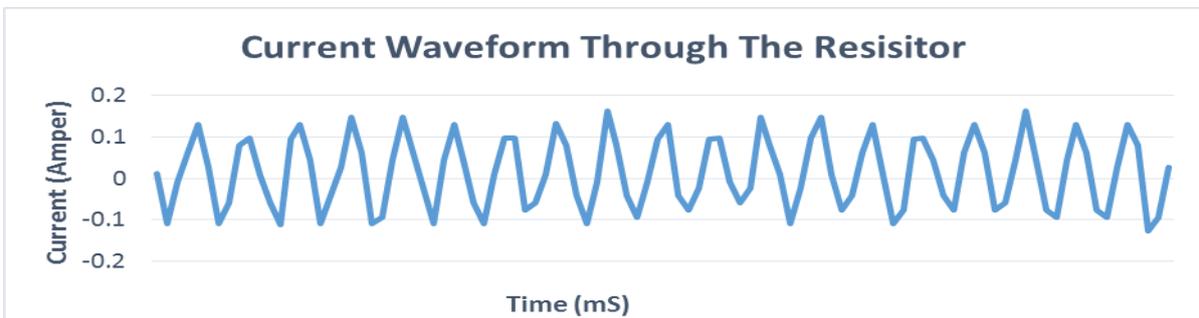
Fig 7. A Graph of current flowing through R1 analysed using Microsoft® Excel
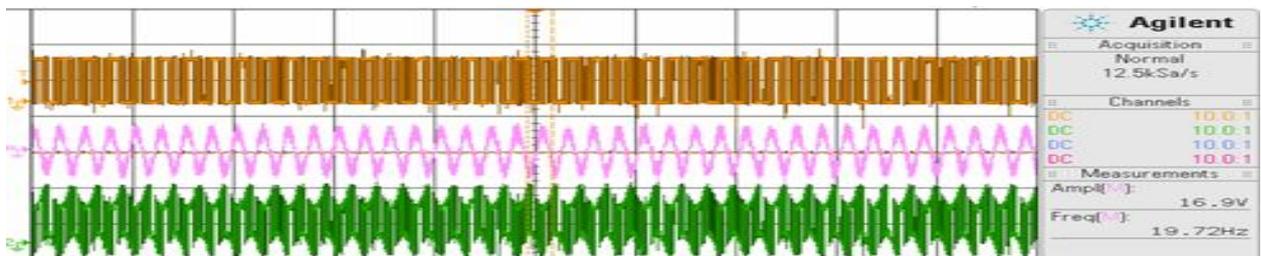
Fig 8: Highest frequency obtained by altering the R22 potentiometer to one of its extremes
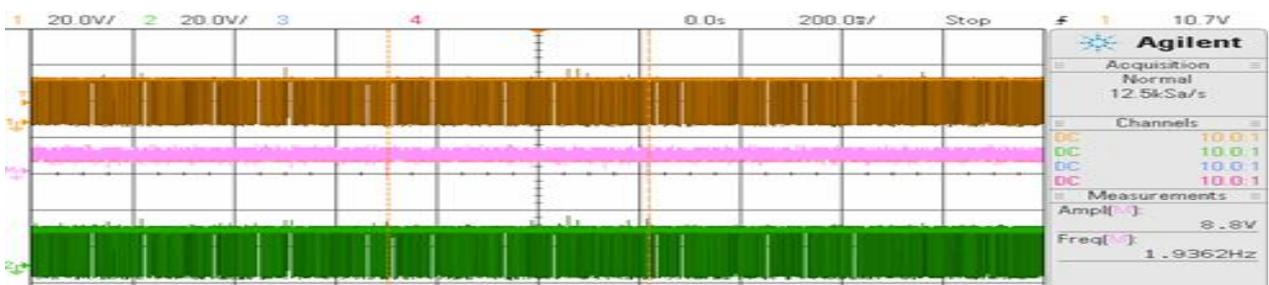
Fig 9: Lowest frequency obtained by altering the R22 potentiometer to one of its extremes
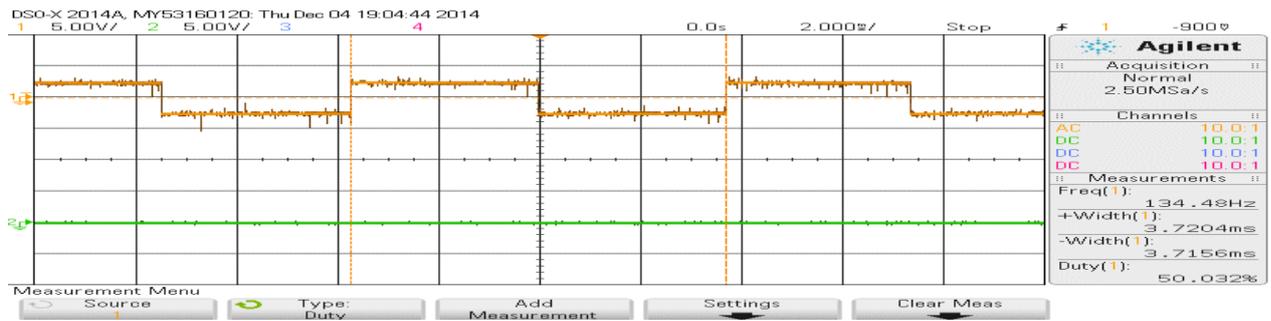
Fig 10. Captured Scope trace for Phase A at 134.48 Hz for motor rotational speed of 2017.
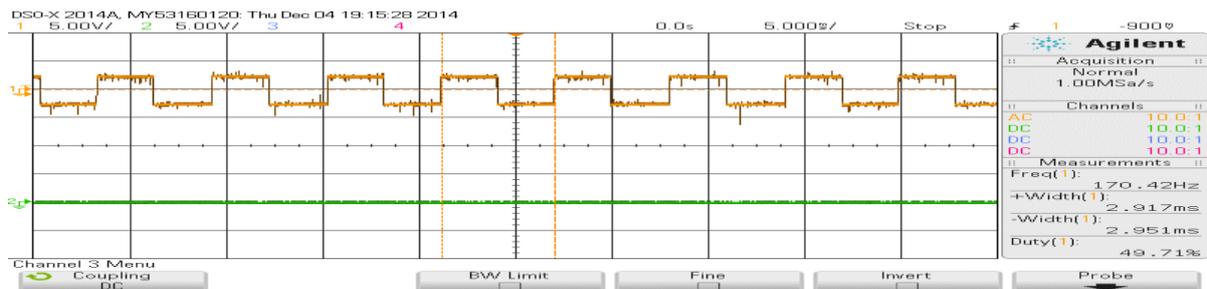
Fig 11. Captured Scope trace for Phase A at 170.42 Hz for maximum motor rotational speed of 2556 rpm.
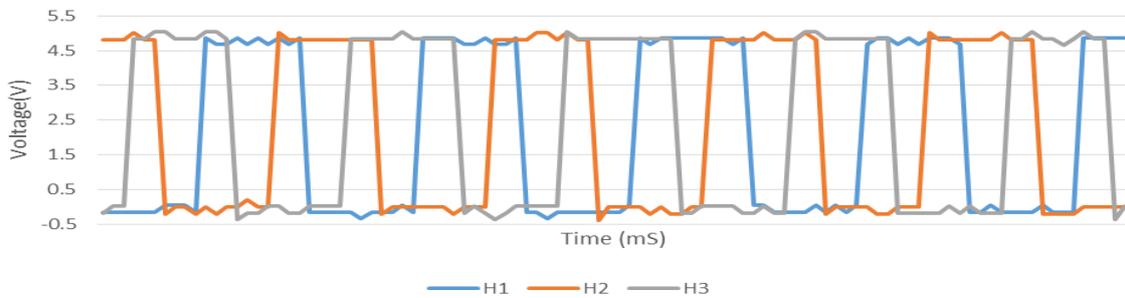
Fig 12. The 3-Phase Hall Effect Sensor Voltage analysed using Microsoft® Excel
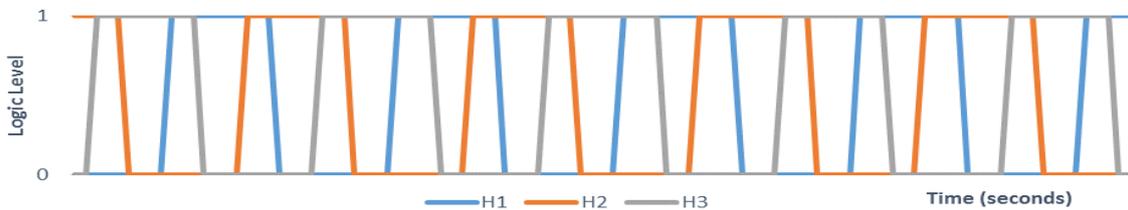
Fig 13. The 3-Bit Hall Effect sensor sequence analysed using Microsoft® Excel
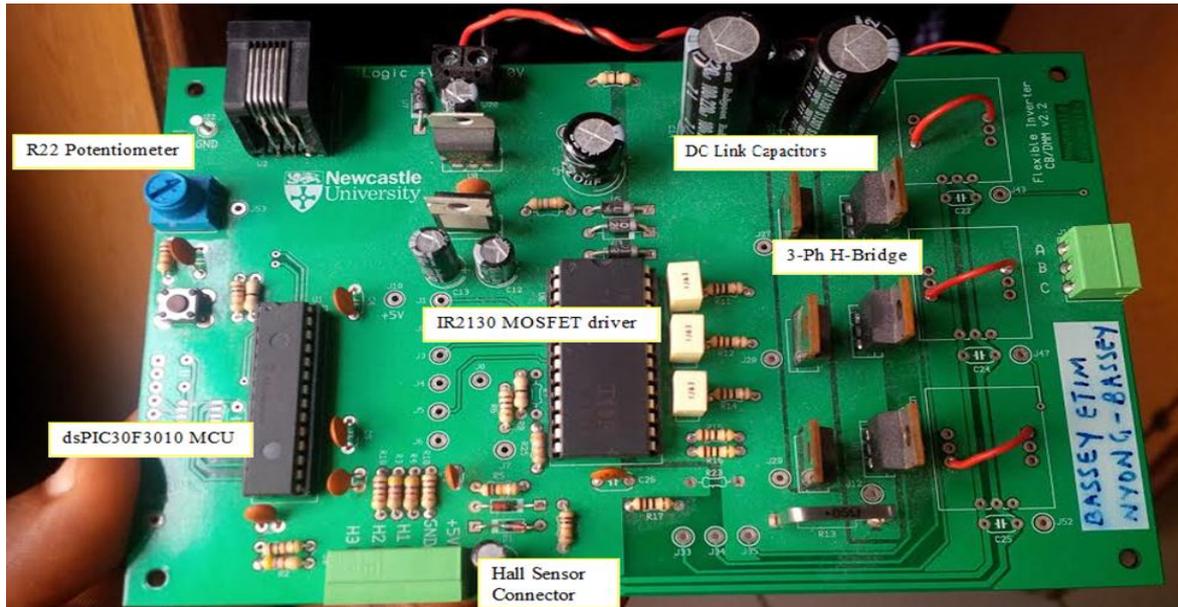
Fig 14. BLDC Speed Control flow chart
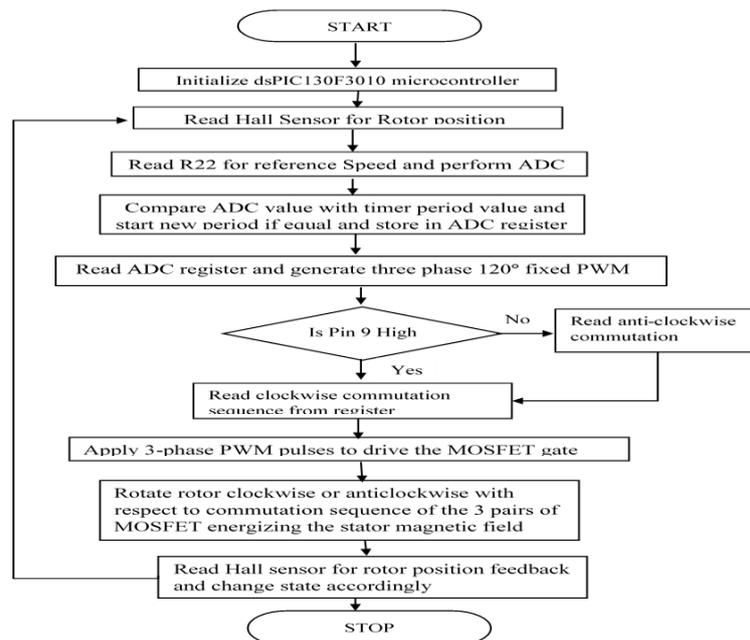
Fig 15. Flexible Inverter Circuit Board
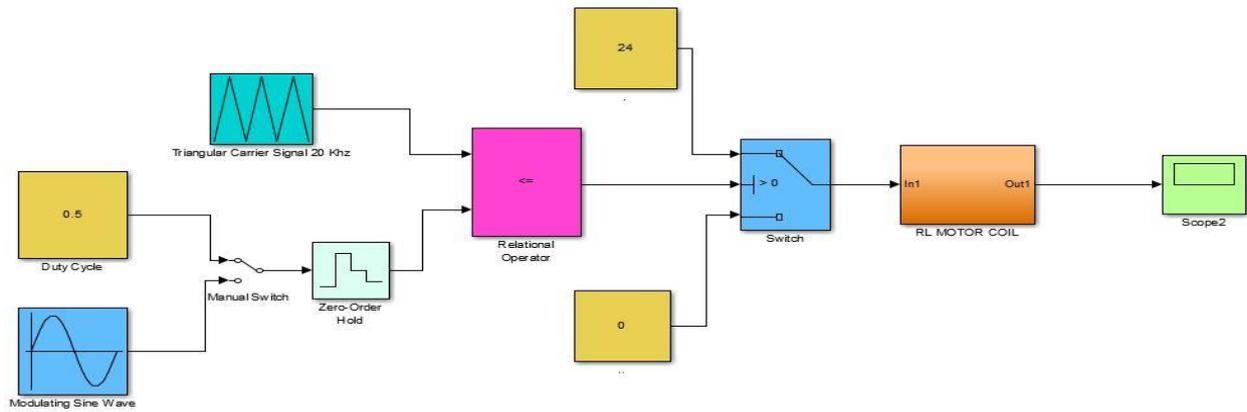
Fig. 16 PWM Modelling of RL Motor Coil for Variable AC or DC Simulation.
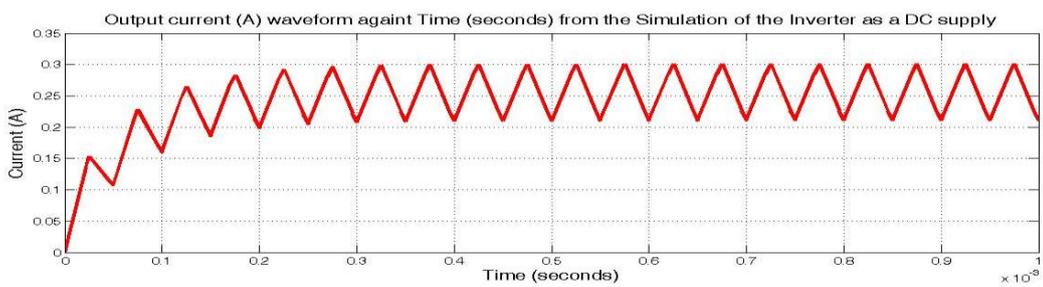
Fig 17. Output current against time: simulation of the inverter as a variable DC supply.
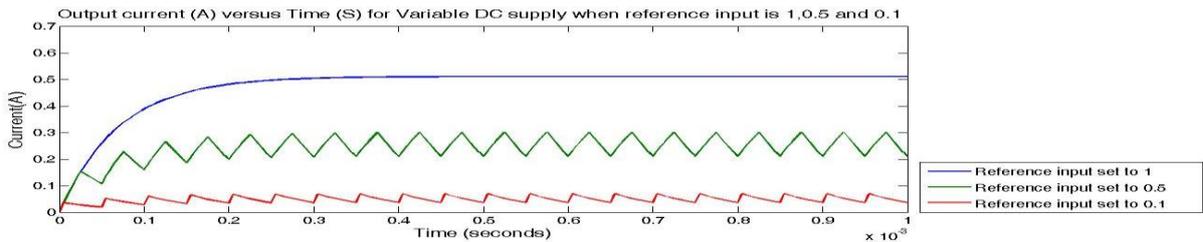
Fig 18. Output current waveform with varying reference input values of 1, 0.5 and 0.2
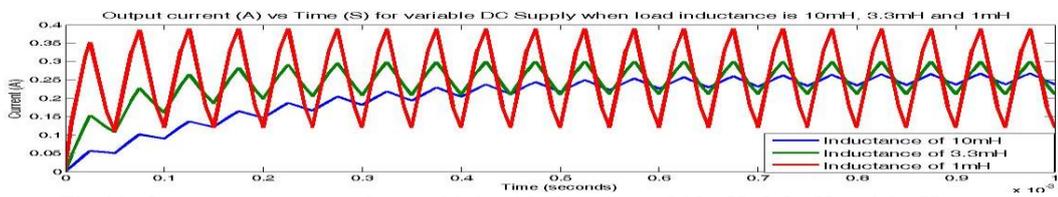
Fig 19. Output current waveform with load inductance of 10mH, 3.3mH and 1mH
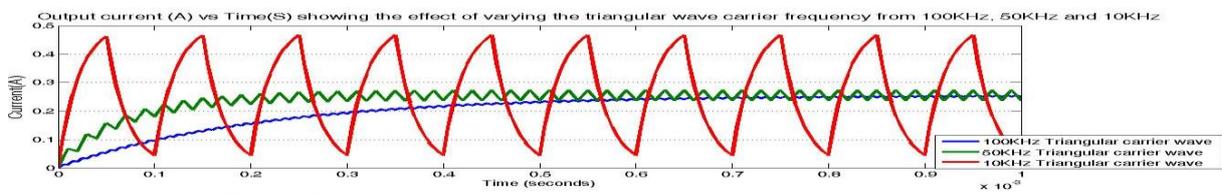
Fig 20. Output current as triangular wave carrier frequency was varied
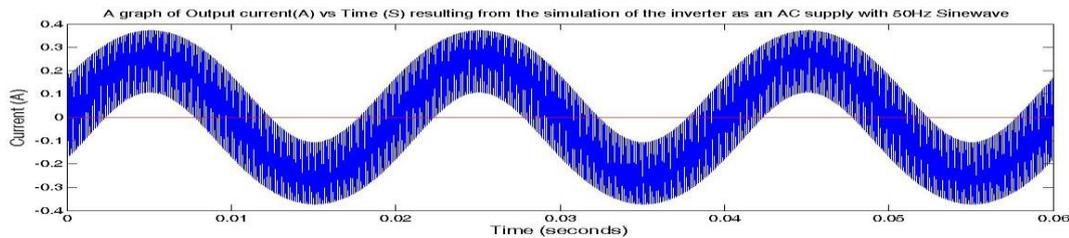
Fig 21. The Inverter Output Current Waveform as an AC supply with 50Hz sinewave input
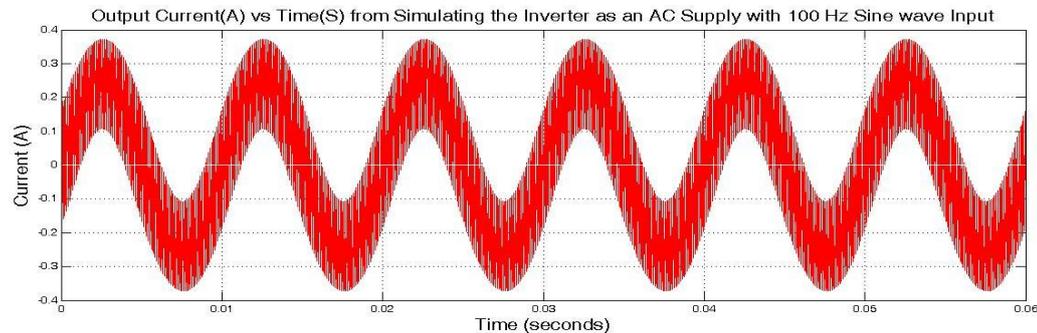

Fig 22. The Inverter Output Current Waveform as an AC supply with 100Hz sinewave input
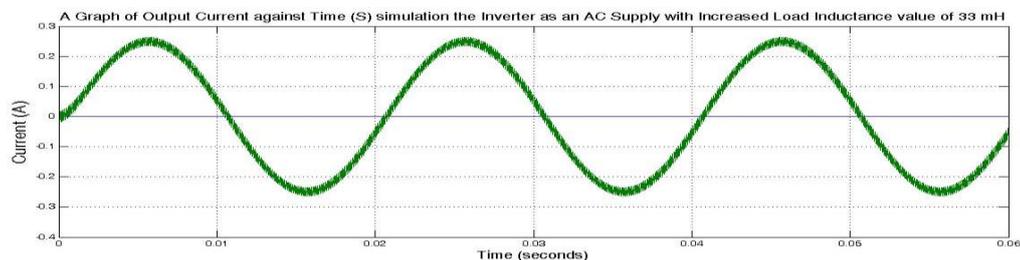

Fig 23. Output Current waveform of increased inductance load of 33mH.

References

[1] Ross, J.N. (1997) *The essence of Power Electronics*, Cornwall, Great Britain: Harnolls limited. Pg 77, 177-180.
[2] Hughes, A. (2009) *Electric Motors and Drives Fundamental, Types and Application,* Oxford Great Britain: Elsevier Limited.pg 357.
[3] Tian, W., 2012. Design of permanent magnet brushless DC motor control system based on dsPIC30F4012. Procedia Engineering, 29, pp.4223-4227.
[4] Janpan, I., Chaisricharoen, R. and Boonyanant, P., 2012. Control of theBrushless DC Motor in Combine Mode. *Procedia Engineering*, *32*, pp.279-285.
[5] Huazhang, W., 2012. Design and Implementation of Brushless DC Motor Drive and Control System. *Procedia Engineering*, *29*, pp.2219-2224.
[6] Application note for DSPIC30F3010 microcontroller. Available at *http://ww1.microchip.com/downloads/en/DeviceDoc/70141F.pdf*(Accessed: 18 March 2016)
[7] *http://electronicdesign.com/power/mosfet-design-basics-you-need-know-part-2* (Accessed: 24th February, 2016).
[8] Chowdhury, D., Chattopadhyay, M. and Roy, P., 2013. Modelling and Simulation of Cost Effective Sensorless Drive for Brushless DC Motor.*Procedia Technology*, *10*, pp.279-286.
[9] Paul, A.R. and George, M., 2011, July. Brushless DC motor control using digital PWM techniques. In *Signal Processing, Communication, Computing and Networking Technologies (ICSCCN), 2011 International Conference on*(pp. 733-738). IEEE
[10] Yedamale, P. (2003) *Brushless DC (BLDC) Motor Fundamentals,* Berkshire, England: Microchip Technology Inc.
[11] Dahidah M. 2015, EEE8075 – Electrical Power and Control Project Notes, Newcastle University
[12] Chern, Y.L., Pan, P.L., Chern, Y.L. and Tsay, D.M., 2010, June. Sensorless speed control of BLDC motor using six step square wave and rotor position detection. In *Industrial Electronics and Applications (ICIEA), 2010 the 5th IEEE Conference on* (pp. 1358-1362). IEEE